Water Science & Technology

A method to identify the weakest link in urban drainage systems

Didrik Meijer [a,b,*], Hans Korving[a], Jeroen Langeveld **IWA**[b,c] and François Clemens-Meyer[d,e]

[a] Deltares, Boussinesqweg 1, 2629 HV Delft, Postbus 177 2600 MH, Delft, The Netherlands
[b] Faculty of Civil Engineering and Geosciences, Delft University of Technology, Stevinweg 1, 2628 CN, Delft, The Netherlands
[c] Partners4urbanwater, Graafseweg 274, 6532 ZV, Nijmegen, The Netherlands
[d] Faculty of Engineering, Department of Civil & Environmental Engineering, Norwegian University of Science & Technology, Høgskoleringen 6, 7491, Trondheim, Norway
[e] SkillsInMotion B.V., Esdoornlaan 11, 3454 HH, Utrecht, The Netherlands
*Corresponding author. E-mail: didrik.meijer@deltares.nl

DM, 0000-0002-1747-0581

ABSTRACT

Urban drainage systems are composed of subsystems. The ratio of the storage and discharge capacities of the subsystems determines the performance. The performance of the urban water system may deteriorate as a result of the change in the ratio of storage to discharge capacity due to aging, urbanisation and climate change. We developed the graph-based weakest link method (GBWLM) to analyse urban drainage systems. Flow path analysis from graph theory is applied instead of hydrodynamic model simulations to reduce the computational effort. This makes it practically feasible to analyse urban drainage systems with multi-decade rainfall series. We used the GBWLM to analyse the effect of urban water system aging and/or climate scenarios on flood extent and frequency. The case study shows that the results of the hydrodynamic models and the GBWLM are similar. The rainfall intensities of storm events are expected to increase by approximately 20% in the Netherlands due to climate change. For the case study, such an increase in load has little impact on the flood frequency and extent caused by gully pots and surface water. However, it could lead to a 50% increase in the storm sewer flood frequency and an increase in the extent of flooding.

Key words: backwater effects, criticality, flow paths analysis, graph theory, linearised hydrodynamics, system performance

HIGHLIGHTS

- An analysis of urban water systems with multiyear rainfall series.
- A combined analysis of subsystems of urban water subsystems.
- A sensitivity analysis of urban water systems in consequence of aging or climate change.
- Comparing flood frequency and flood extent caused by capacity reduction of urban water subsystems.
- Flow path analysis from graph theory instead of hydrodynamic model simulations.

1. INTRODUCTION

Urban drainage systems, which prevent pluvial flooding, expand as cities grow. From this, it follows that urban redevelopment projects result in adjustments of these systems. These are long-term processes and urban drainage systems have often 'grown organically' to their current state. During the construction period, substantial change was observed in laws, regulations, the related design standards and design criteria, available techniques, personnel and material costs and external conditions such as climate and water use (Preston & van de Walle 1978; Geels 2006). As a result, urban drainage systems and their subsystems have their own specific characteristics in terms of storage and discharge capacity. These characteristics reflect the dominant dynamics at their specific temporal (minutes, hours and days) and spatial scales (building, street, neighbourhood and city) (Langeveld & Schilperoort 2019).

The performance of the urban water system depends on the functioning of its subsystems, such as gully pots, storm sewers and surface water. The combination of storage and discharge capacity determines the drainage capacity of a subsystem. The interactions between the subsystems affect the capacity of the system (Sommer *et al.* 2009; Langeveld & Schilperoort 2019;

Ferguson & Fenner 2020). Backwater effects may change the internal boundary conditions between subsystems, resulting in a reduction of the hydraulic capacity of the subsystems. A delayed discharge from a storm water system may result in increased water levels in the surface water system at an undesirable time. The study by Reyes-Silva *et al.* (2020) shows that subsystem interactions and network performance are under pressure in a consequence of:

- Increasing load as a result of urbanisation, population growth and densification.
- Deterioration as a result of aging (and lack of maintenance) resulting in a decrease in capacity.
- Terrorist attacks.

Each network connection contributes differently to the network's performance in terms of preventing flooding by draining water. Some connections only influence the performance of the network in their immediate vicinity, whereas other elements influence the performance of (almost) the entire network. Knowledge of an element's contribution to network performance can be applied when (re)designing urban drainage systems or when making decisions on asset management (van Riel 2016). However, integrated urban drainage systems are rarely analysed in practical cases. The main reasons for this are summarised as follows:

- In many countries, individual parts of the systems are managed by different organisations (e.g. in the Netherlands, surface water by water boards, drainage systems by municipalities and large rivers by the national government).
- Tools applied for subsystems are not always mutually aligned (Tscheikner-Gratl *et al.* 2019).
- Current methods for integrated analysis are complex, time-consuming and demand simplifications. The current complex software tools for 1D-2D simulations require a large processing capacity. Because input data are lacking the results are not always reliable (Tscheikner-Gratl *et al.* 2019).

From this, it follows that in practical cases, integrated analyses are rarely used due to the time-consuming calculation and the expertise needed to evaluate the model results. In order to reduce the calculational effort design storms can be applied instead of precipitation series. Alternatively, the network can be simplified by excluding manholes and/or pipes. However, simplification of the network may reduce the usability of the flood simulation results (Fischer *et al.* 2009; Yang *et al.* 2018) as it often implies a reduction in spatial resolution. The outcomes are not always sufficiently accurate to determine whether the (sub)systems match in terms of storage and discharge capacity. Replacing rainfall series with (a series of) design storm(s) prevents an accurate statistical analysis of the behaviour of the subsystems (Vaes *et al.* 2009).

Ferguson & Fenner (2020) and Qiang *et al.* (2021) showed that backwater effects in storm sewers affect the extent and duration of flooding in the urban areas. This means that the integration of storm water and surface water models is necessary in the analysis of urban drainage models. A main conclusion from the work of Tscheikner-Gratl *et al.* (2019) is that the applied spatial and temporal resolution in models are a limiting factor for model integration. Despite the importance of coupled systems analysis and the challenges it poses, little attention has been paid to this topic in the literature.

In the review of the adaptation of drainage networks to climate change of Kourtis & Tsihrintzis (2021), the subject is not mentioned. The literature review on neurocomputing by Zounemat-Kermani *et al.* (2020) lists examples of modelling of surface water and storm sewers but places little focus on integrated systems. There are many papers about 1D-2D modelling (storm sewer and overland flow) but even these pay little attention to the dependencies between storm sewers and surface water. The observation of Bach *et al.* (2014) that 'despite greater inter-sector communication, practice remains fragmented' seems still valid.

We developed the graph-based weakest link method (GBWLM) for analysing impacts on the performance of urban drainage systems as a result of changes in load or system degradation, which is presented in this paper. The GBWLM combines the structure of the network with flow path analyses which replace the hydrodynamic equations. The GBWLM and the Achilles approach are used to quantify the flood extent and frequency for a case study and the results are compared and presented. The extent and frequency of urban flooding as determined by hydrodynamic models and the GBWLM are similar for the case study. The results show that the performance of the urban water system decreases as the subsystem's performance decreases. For rainwater sewers, this is already visible from a capacity reduction of 10–20% and for surface water only from a capacity reduction of 70–80%. Based on the case study, it was concluded that the GBWLM can be applied to systems where performance is determined by discharge capacity or storage capacity.

2. METHODS

2.1. The Achilles approach

The performance of the urban water system decreases as a consequence of increasing loads and deterioration. The degree of performance degradation depends on which elements deteriorate or are subjected to changes in loads. Some (groups of) elements are more critical to system performance than others. The performance of the whole system is affected if the performance critical elements decline. A generally applicable method to determine the criticality of elements in networks is shown in Figure 1. This method has been adapted from the Achilles approach (Möderl et al. 2009; Mair et al. 2012) and the percolation theory (Stockmayer 1944; Broadbent & Hammersley 1957; Stauffer & Aharony 1991; Sahimi 1994). This method aims to quantify the effect of a reduced capacity of an element to the system's performance level as a whole (Möderl et al. 2009; Mair et al. 2012). The Achilles approach can be used to determine vulnerable sites of (water) infrastructure. The outcomes of a hydrodynamic model are used for the determination of vulnerabilities.

The Achilles approach can be used to evaluate the contribution of subsystems or groups of elements to the functioning of the entire system, for example, an urban water system consisting of gully pots, storm sewers and surface water. For the identification of vulnerabilities, the outcomes of a hydrodynamic model are used (hydrodynamic model method, HMM). First, a simulation is done with the original model in which all conduits function well. After this, the diameters of the conduits are one by one reduced to zero to simulate a blockage. For every blocked conduit, a simulation is carried out, so the number of simulations to be made is equal to the number of conduits plus one. The results are compared based on the increase in calculated ponded volumes. The reduced conduit diameter causing the largest increase in ponded volume is identified as the most critical pipe.

2.2. Graph-based weakest link method

The performance of an urban water system depends on the load and the system's response characteristics. The latter may be affected by the interactions between the various subsystems and may change over time or even during an event. The impact of changes in load or capacity depends on the storage and discharge capacities of the subsystems, which differ. The GBWLM
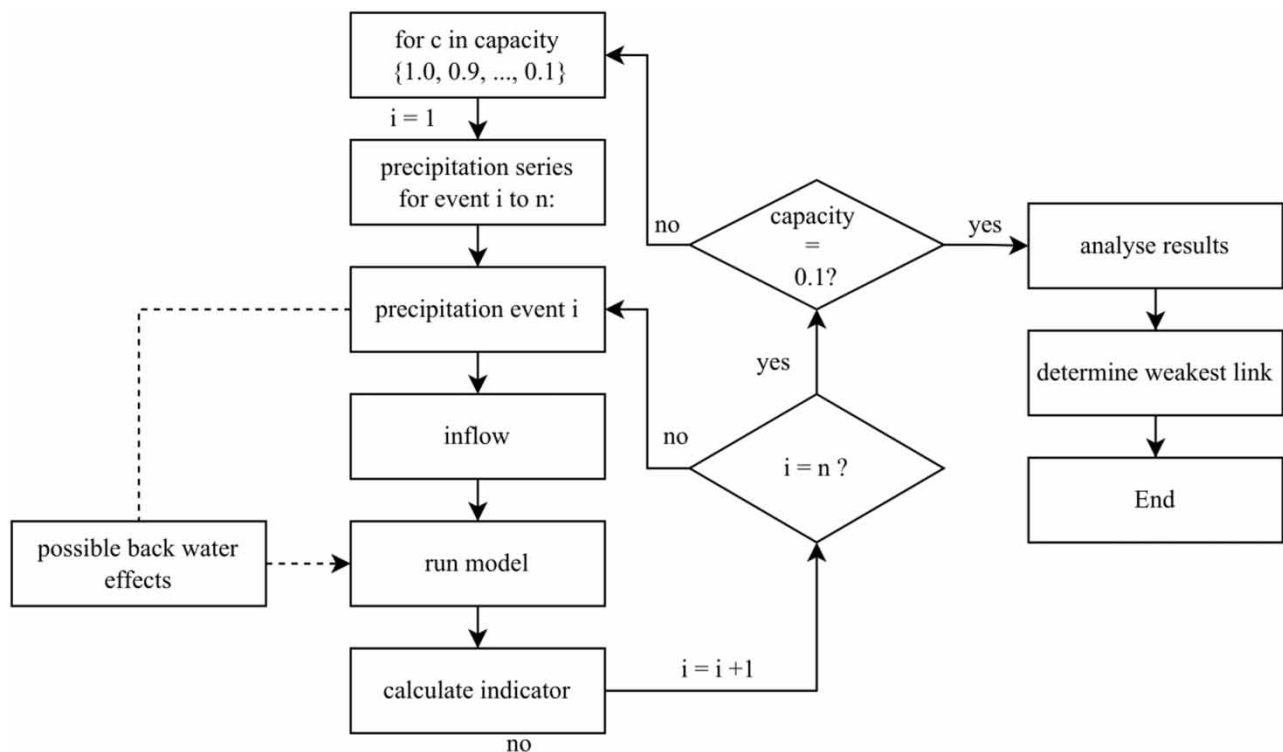

Figure 1 | General overview of the Achilles approach applied to urban drainage systems.

has been developed to analyse, applying multi annual precipitation series, integrated urban water networks at three levels of subsystems: gully pots, storm sewers and surface water systems. The metrics applied to evaluate the system's performance are the flood frequency and flooded area. The general outline of the GBWLM is shown in Figure 2. The various components are described in some detail in the following sections.

The urban drainage system is tested with a rainfall series (see Section 2.3. precipitation load on the subsystems). The discharge of water via the gully pots, storm sewer and surface water is analysed with a flow path analysis in combination with a water balance (see section Analysis of network performance with flow path analysis). The flow path analysis replaces the hydrodynamic model normally used. To apply flow path analyses, the networks are schematised as digraphs consisting of multiple layers (see Section 2.5. Graph schematisation of storm water and surface water networks). For each edge of the digraph, a cost and capacity are determined based on linearised hydrodynamics (see. Section 2.7. Costs and capacity of the edges). Finally, the capacity of the subsystems is reduced incrementally and its effects are analysed (see Section 2.8. Capacity reduction and effect).

2.3. Precipitation load on the subsystems

The test load applied is a multiyear precipitation series that is subdivided into mutually independent events (see, the precipitation blocks at the top of the three columns in Figure 2). A model for rainfall-runoff is omitted for the sake of simplicity. As a result, inflow is equal to precipitation volume at all times. Events are considered to be mutually independent when the initial conditions of the system are identical for each event (i.e. the time for emptying the system after a storm event has to be considered as this determines the initial filling of the system for the next event. These events are considered independent only when the time-gap between the time windows in which precipitations occur is larger than the time needed to empty the system). The characteristic system response times are determined and used to divide the series into separate, independent events.
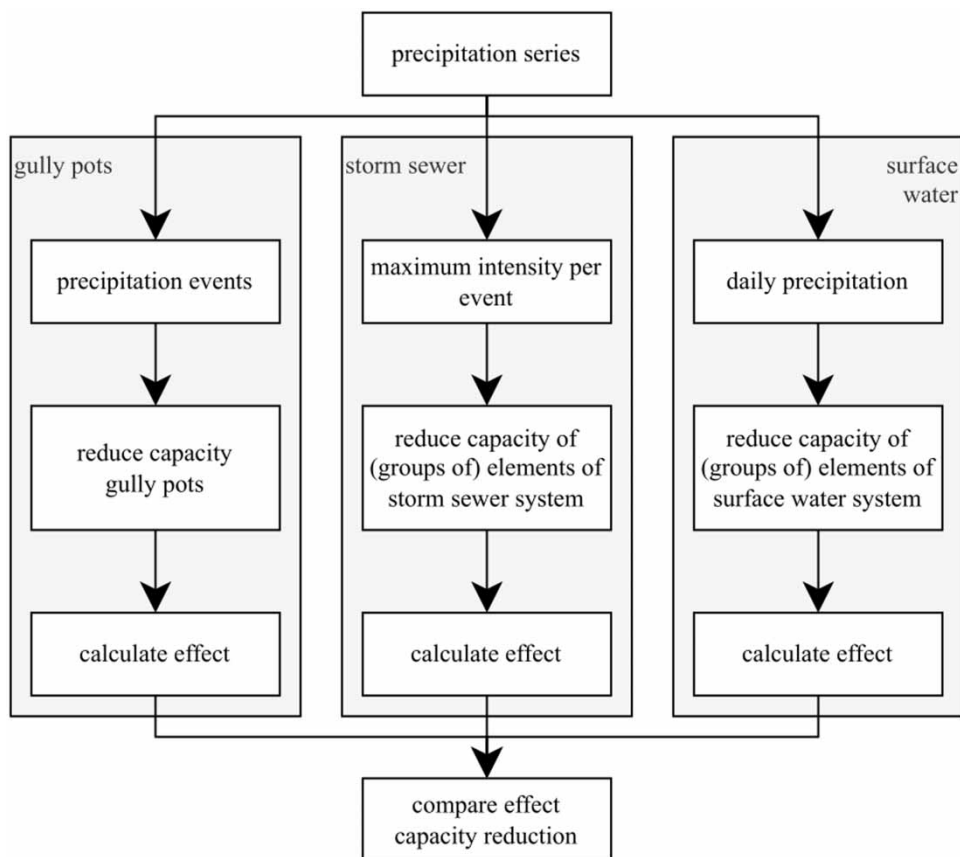

Figure 2 | The GBWLM process for urban drainage systems focused on gully pots, storm sewers and surface water systems.

The critical precipitation load of the subsystems depends on their primary function (storage or discharge). The leading principles (in flat areas) are the following:

- Gully pots: exceeding discharge capacity (rainfall intensity).
- Storm sewers: exceeding discharge capacity (rainfall intensity).
- Surface water systems: exceeding storage capacity (rainfall volume).

The inflow and outflow of subsystems are interdependent. The maximum drainage capacity of gully pots affects the maximum inflow of the storm sewers. In addition, the cumulative outflow of the storm sewer results in a cumulative inflow of the surface water system (for more details, see Supplementary material).

2.4. Analysis of network performance with flow path analysis

The GBWLM is based on the Achilles approach. The hydrodynamic models have been replaced by water balances and flow path analysis. The GBWLM shares the flow path analyses with the graph theory method (GTM) for pressurised systems (Meijer *et al.* 2020) and gravity-driven systems (Meijer *et al.* 2018). The outcome of the GBWLM is the flooded area, flood frequency and the outcome of the GTM is the criticality of the network elements.

The functioning of urban drainage systems is affected by the available discharge and storage capacity. The discharge capacity is used to evaluate the performance of the gully pots and storm sewers. The surface water system performance is evaluated based on the combination of discharge and storage capacity.

The gully pots are represented as a reservoir with an outflow. The storm sewers and surface water system networks are described as digraphs. The performance of the networks is analysed using a flow path analysis. All connections in the network must be given a capacity and a cost, to perform a flow path analysis. Capacity is the amount of water that can be drained through a connection. The cost is the amount of energy (head loss) required to drain the water (see, Meijer *et al.* 2018). An analysis is performed to determine how the inflowing water can be discharged to the outfall points at the lowest possible cost. The manholes in a storm sewer are the inflow points (sources) and the storm sewer outfalls (SSOs) are the outflow points (targets). The SSOs are the sources in the surface water system and the final pumping station is the target.

The minimum cost flow algorithm (min_cost_flow) of the Networkx module in Python (Hagberg *et al.* 2008; NetworkX Developers n.d.) is applied for the flow path analysis and the evaluation of the consequences of a capacity reduction in networks. The algorithm can be applied to a digraph in which the edges have both a cost and a capacity. The nodes send or receive some amount of flow. The algorithm calculates the minimum costs for a flow that satisfies the demands of all nodes. That means that for each node, the net inflow or outflow is equal to the demand of that node.

The inflow and outflow of the subsystems are dynamic. The inflow of the gully pots corresponds to the applied rainfall series multiplied with the runoff area. The sewer systems are analysed using the maximum gully pot outflow per event, the drainage capacity of the surface water system is analysed based on the daily outflow (based on the complete precipitation series) of the sewer system and the discharge of the ground water system and the storage in the surface water system using a water balance with a time step of 1 day.

The GBWLM is applied to analyse the consequences of a reduced discharge and storage capacity in the subsystems. The consequences of a reduced discharge capacity have been analysed with both the Achilles approach and the GBWLM. We have analysed whether the rising of the surface level has a backwater effect on the functioning of the storm sewer system. We also analysed whether it leads to flooding from the storm sewer system (see Figure 3).

2.5. Graph schematisation of storm water and surface water networks

The design of the subsystems in the GBWLM is tuned to the characteristics of the systems and the leading principle. A gully pot is represented as a reservoir with an outflow. The storm sewers and surface water systems are described as digraphs (Layer-1 in Figures 4 and 5). The nodes represent manholes and the edges represent conduits in storm sewer digraphs. In surface water digraphs, the nodes correspond to the watercourses between two structures and the edges of the structures (weirs, orifices and pumps).

2.5.1. Surface water system

A copy of Digraph-1 is created (Digraph-2) for the surface water system. The two digraphs, when combined, form an object referred to as a layered graph (Layer-1 = Digraph-1, Layer-2 = Digraph-2; Figure 4). Layer-2 is used as a bypass to drain the water if the capacity of Layer-1 is insufficient. The bypass is used to ensure that the algorithm used (minimum cost flow
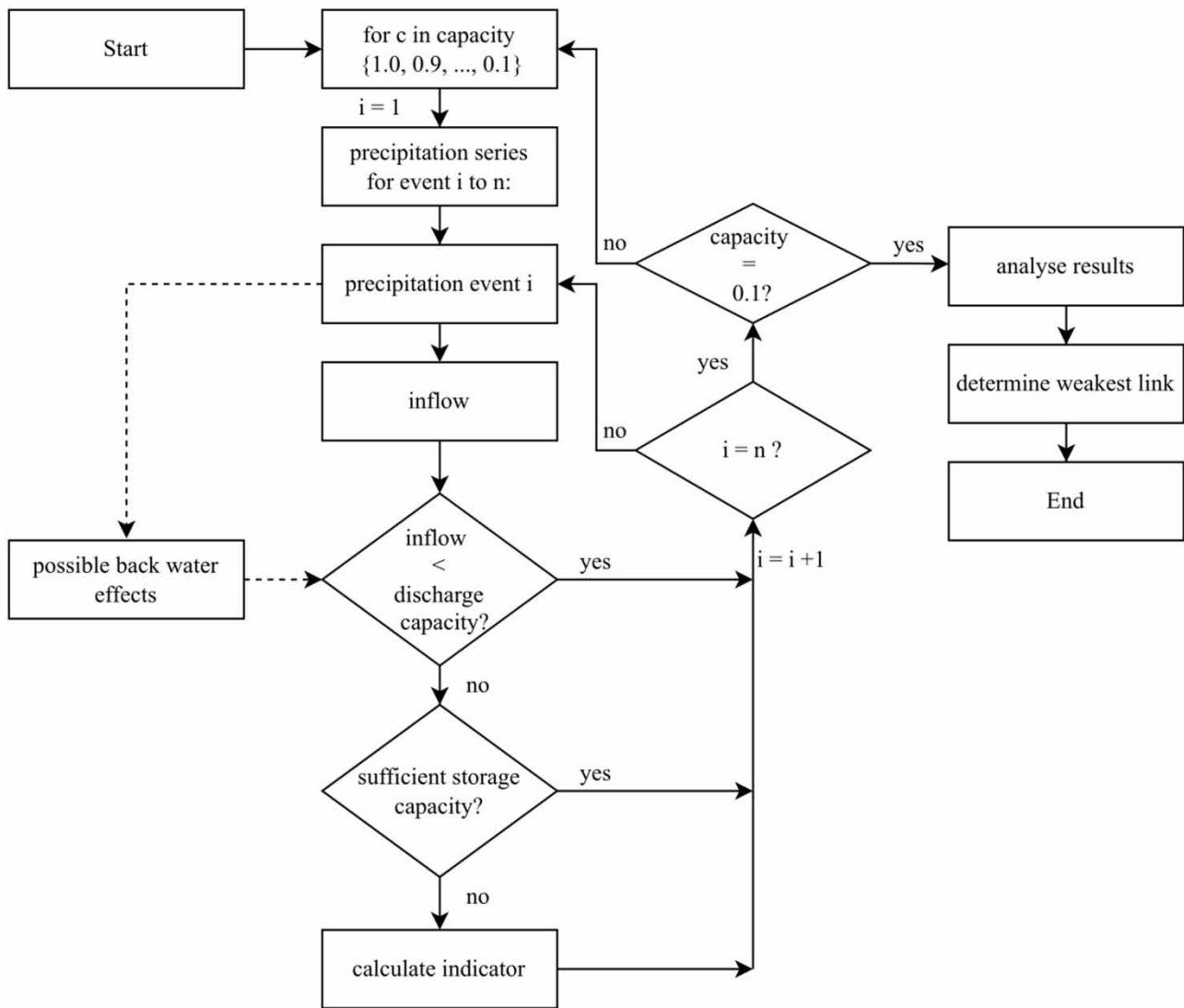
Figure 3 | General overview of the hydrodynamic model-based weakest link method applied to urban drainage systems.
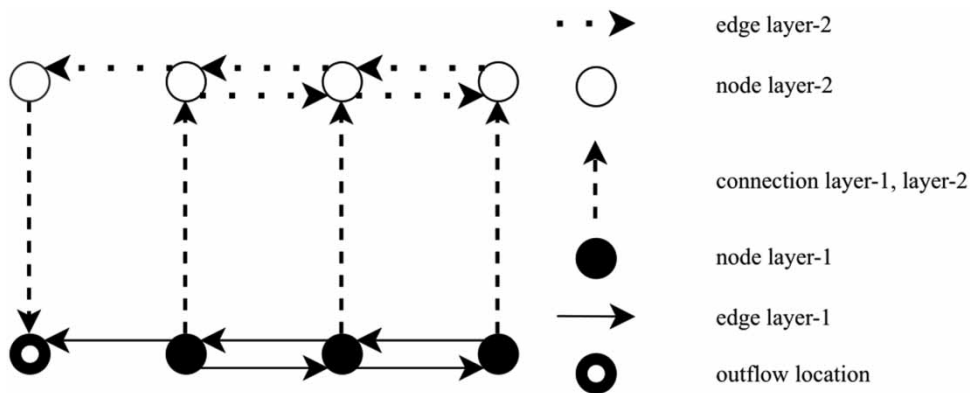

Figure 4 | Overview of the edge types in the surface water component of the GBWLM. Layer-1 represents the structure of the network in which the nodes represent manholes watercourses. Edges correspond to the structures. Layer-2 is used when the capacity of Layer-1 is exceeded and indicates rising water levels in the surface water system.
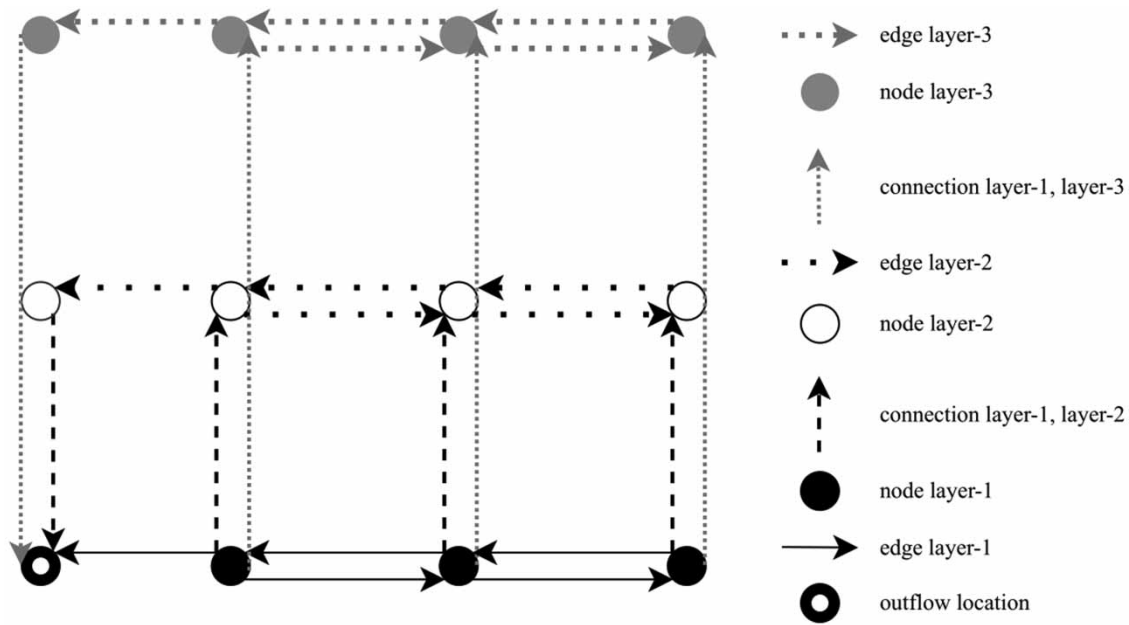
Figure 5 | Overview of the edge types in the storm sewer component of the GBWLM. Layer-1 represents the structure of the networks in which the nodes represent manholes. Edges correspond to the pipes and structures. Layer-2 is used when the capacity of Layer-1 is exceeded and indicates flooding. Layer-3 is a bypass in case the capacity of the links between Layer-1 and Layer-2 is exceeded.

algorithm) always finds a solution. The layers are connected to the nodes (structures). Each node of Layer-1 is connected with its copy in Layer-2. The direction of the connection between the layers at the outflow location(s) is from Layers 2 to 1. The direction between the layers at the other nodes (structures) is from Layers 1 to 2.

For the surface water system, a water balance is used at each node to store the water that cannot be drained via the structures. The available storage is determined for the watercourses between two structures with the following equation:

$$
\left.
\begin{aligned}
\Delta t \cdot Q_{\text{in}} + S_{t-1} > \Delta t \cdot Q_{\text{structure}} &\rightarrow Q_{\text{out}} = Q_{\text{structure}}, \\
S_t &= S_{t-1} + \Delta t \cdot Q_{\text{in}} - \Delta t \cdot Q_{\text{out}} \\
\Delta t \cdot Q_{in} + S_{t-1} \le \Delta t \cdot Q_{\text{structure}} &\rightarrow Q_{\text{out}} = Q_{\text{in}} + \frac{S_{t-1}}{\Delta t} \\
S_t &= S_{t-1} + \Delta t \cdot Q_{\text{in}} - \Delta t \cdot Q_{\text{out}} = 0
\end{aligned}
\right\}
\tag{1}
$$

where Q_{out} is an outflow of the surface water node (m³/s), Q_{in} is the inflow of the surface water node (m³/s), $Q_{\text{structure}}$ is the maximum discharge capacity structure (m³/s), Δt is the time interval (s) and S_t is a storage in the surface water node at time-step t (m³).

2.6. Storm sewer system

Two copies of Digraph-1 are created (Digraphs 2 and 3) for the storm sewer system. The nodes in Layer-1 represent the manholes. The edges represent the conduits of the storm sewer system. Each node (manhole) of Layer-1 is linked to the copy of this node in Layer-2 (connection L1–L2) and Layer-3 (connection L1–L3). The nodes of the layers are connected with an edge in the opposite direction at the outflow locations (connections L2–L1 and L3–L1 instead of connections L1–L2 and L1–L3). Layer-2 is used to drain the water when the capacity of Layer-1 is insufficient. Layer-3 is used as a bypass to drain the water when the capacity of Layer-1 and the connections L1–L2 are insufficient (Figure 5). This bypass does not refer to a physical element but is necessary to ensure that the algorithm can always be applied. The use of three layers allows one to limit the capacity of the connection L1–L2 and still always arrive at a solution to the minimum cost flow algorithm via Layer-3.

The capacity limitation of L1–L2 corresponds to the pressure in a manhole during flooding. When the capacity of L1–L2 is not limited, the water that cannot be drained through Layer 1 can flow through a limited number of manholes to Layer 2,

which results in an underestimation of the flood extent. Because of the applied cost, the water always flows from L1–L2 before edge L1–L3 is used. As a result, the node is already marked as flooded.

2.7. Costs and capacity of the edges

The costs of most of the edges in the GBWLM are derived from the head loss (see Meijer *et al.* 2018) except for the connections between the layers. The capacity of the edges is based on linearised hydrodynamics. The general process to determine the capacity of the pipes is described in the next section. To determine the capacity or costs for the edges between the graph layers, an additional analysis is required or an exception can be made. These are described in the sections after the linearised hydrodynamic section.

2.7.1. Linearised hydrodynamics in the GBWLM

Hydrodynamics are linearised to estimate the capacity of the pipes and the costs of the connections between layers of the graph. The quadratic hydraulic gradient equation (Equation (2)) has been simplified to a linear relationship (Equation (3)). The maximum capacity of each pipe is computed (Equation (2)) based on the maximum available hydraulic gradient. $\alpha_{\text{quadratic}}$ is based on the Chézy formula. α_{linear} is determined for each pipe by linearising the discharge (between zero and the maximum pipe capacity) and the maximum available hydraulic gradient (Equation (3)):

$$I = \alpha_{\text{quadratic}}Q^2 \tag{2}$$

$$I = \alpha_{\text{linear}}|Q| \tag{3}$$

$$I = \frac{R}{C^2 A^2}Q^2 \tag{4}$$

where I is the hydraulic gradient (–), Q is the discharge (m³/s), $\alpha_{\text{quadratic}}$ is a quadratic hydraulic parameter (s²/m⁶), α_{linear} is a linear hydraulic parameter (s/m³), C is the Chézy coefficient (m^{0.5}/s), A is the wet surface of the pipe (m²) and R is the hydraulic radius (m).

The process of linearisation in the GBWLM comprises the following steps:

1. Calculate the cost of the pipes based on the head loss.
2. Calculate the available hydraulic gradient. The available gradient for conduits depends on the crest level or surface water level of the outflow point, street level and path length and is determined as follows:
   i. The shortest paths of all nodes to the closest outflow points are calculated with the Dijkstra algorithm for Digraph-1 (Layer -1 in Figure 6) (Dijkstra 1959).
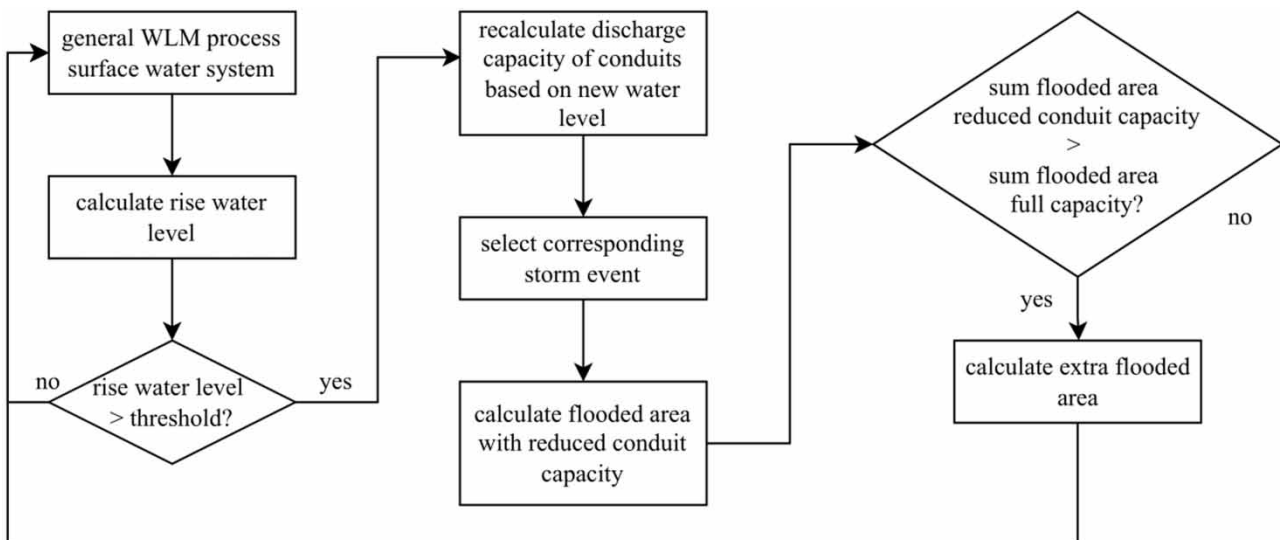

Figure 6 | Process of the surface water component of the GBWLM.

   ii. The minimum available hydraulic gradient is determined for each manhole. The differences between ground level and crest level are divided by the path length without taking into account the available gradients of the other manholes.

   iii. The available hydraulic gradient is recalculated for each manhole (from the smallest to the largest available hydraulic gradient from Step ii), taking into account the gradients of the other manholes. If a path crosses a path with a known hydraulic gradient, the hydraulic gradient is computed between the level of the gradient line at the junction, the street level and the path length.

3. Calculate the pipe capacity with Equation (2).
4. Calculate α_{linear} with Equation (3).
5. Determine the runoff area that discharges via a pipe. The paths that include a pipe are selected. The runoff area of all starting nodes (sources) of these paths is summed.
6. Determine the costs between connections for Layers 1 and 2. The costs are equal to the freeboard (ground level minus water level) of all manholes, which corresponds to the static head loss. The water levels are calculated using an iterative process. The discharge and corresponding hydraulic gradient (Equation (3)) in every pipe are calculated by multiplying the runoff area that drains via a pipe (Step 5) by low rainfall intensity. Starting at the node with the smallest available hydraulic gradient, the water levels are calculated on the path from the closest outfall based on the discharge, Equation (3) and the length of the pipe (see Step 2(c)). If the water level is below ground level at all manholes, the rainfall intensity is increased until the water level is above ground level at one or more manholes. The water levels calculated with the last intensity at which no floods occur are used to calculate the freeboard for every manhole.

2.7.2. Costs of the connections between the layers

The connections between the layers ensure a path through which all the water can always be drained. The connections between the layers may only be used if no other outlet route is available. Therefore, the cost should be equal to the total cost of pipes in Layer-1 (see Table 1).

2.7.3. Structures (edges)

All the structures in the storm water sewers and surface water systems are made of multiple sub-connections in order to increase capacity with increasing head loss. Small changes in head loss can result in large changes in the hydraulic capacity of structures (and especially weirs). The relationship between the capacity and cost (head loss) of a structure is derived from its characteristics. The head loss is incrementally increasing. For each head loss, a sub-connection is added to the graph. The cost of the sub-connection is equal to its head loss. For sub-connection 1, the capacity is equal to the capacity of the corresponding head loss. For the other sub-links (i in two to n), the capacity is equal to the capacity of the corresponding head loss of sub-connection i minus the capacity of the corresponding head loss of sub-connection i–1 (see Table 2).

The capacity and costs of all link types of the GBWLM are summarised, respectively, in Tables 3 and 4.

2.8. Capacity reduction and effect

2.8.1. Gully pots

The gully pot capacities are reduced by decreasing the design discharge capacities by a certain percentage (10–90% in 10% increments). The results of the gully pots can be evaluated (see left column of Figures 2 and 3). The number of events in which the discharge capacity is less than the rainfall intensity (which is identical to the runoff intensity as no rainfall-runoff model is

Table 1 | Costs and capacity of the bypass edges

Subsystem	Edge type	Capacity	Costs
Surface water	Connection Layers 1 and 2	Equal to the total inflow	Total cost of the edges in Layer 1
Storm sewer	Connection Layers 1 and 2	Default value depending on the flood characteristics	The sum of costs of all edges of Layer-1 and the freeboard at the location of the connection (manhole)
Storm sewer	Connection Layers 1 and 3	Equal to the total inflow	Total cost of the edges in layers 1 and 2

Table 2 | Costs and capacity of structures

Sub-connection of structure	Head loss (m)	Costs	Total capacity structure (m³/s)	Capacity sub-connection structure (m³/s)
1	0.01	0.01	$Q = \alpha 0.01^\beta$	$Q = \alpha 0.01^\beta$
2	0.02	0.02	$Q = \alpha 0.02^\beta$	$Q = \alpha 0.02^\beta - \alpha 0.01^\beta$
3	0.03	0.03	$Q = \alpha 0.03^\beta$	$Q = \alpha 0.03^\beta - \alpha 0.02^\beta$
etc.	…	…	…	…

Table 3 | Overview of the capacity of the edges in the digraphs

Edge type	Capacity storm sewer	Capacity surface water
Layer-1	$Q = \alpha H^\beta$	$Q = \alpha H^\beta$
Layer-2	$Q = \alpha H^\beta$	Total inflow
Layer-3	>Total inflow	Not applicable
Connection L1–L2	Default value for more details see Section 2	Total inflow
Connection L1–L3	Total inflow	Not applicable
Connection L2–L1	Total inflow	Total inflow
Connection L3–L1	Total inflow	Not applicable

Table 4 | Overview of the costs of the edges in the digraphs of the GBWLM

Edge type	Costs storm sewer	Costs surface water
Layer-1	Head loss	Head loss
Layer-2	Head loss	Head loss
Layer-3	Head loss	Not applicable
Connection L1–L2	Sum costs of edges in layer-1 + freeboard	Sum costs of edges in layer-1
Connection L1–L3	Sum costs of edges in layer-1 and layer- 2	Not applicable
Connection L2–L1	0	0
Connection L3–L1	0	Not applicable

used) is counted per gully pot and multiplied with the runoff area of the gully pot. This results in an estimation of the flooded area and the flood frequency.

2.8.2. Storm sewers

The capacity of the storm sewer is reduced by decreasing the capacity of all edges by a certain percentage (10–90% in 10% increments). The consequences of a capacity reduction in the sewer system are evaluated using the function min_cost_flow of the Networkx module in Python (Hagberg *et al.* 2008). This function determines the flow paths having minimum costs of all nodes to the central outflow point; this is performed for each event (see the centre column of Figures 2 and 3). Water flows from the nodes of Digraph-1 via the edges to the central outflow point. Manholes are labelled as flooded if the water flows through a Layers 1–2 edge. The flooded area is set equal to the runoff area of the connected gully pots.

2.8.3. Surface water system

The capacity of the surface water system is reduced by decreasing the capacity of all edges by a certain percentage (10–90% in 10% increments). The effects of a reduction in the surface water system are determined in two steps: (1) the water levels are calculated (Figure 3); (2) if these exceed a threshold, then the impact on the storm sewer is calculated (backwater effect, Figure 6).

2.9. Similarities and differences with the graph theory method

The GBWLM shares the flow path analyses with the GTM for pressurised systems (Meijer *et al.* 2020) and the GTM for gravity-driven systems (Meijer *et al.* 2018) but is substantially different. The main characteristics of the three methods are summarised in Tables 5 and 6 to clarify the differences between the methods. The tables show that the costs of edges are derived from the head loss in both the GBWLM and GTM. The GBWLM and the GTM differ on the components: outcomes (flood frequency extent versus ranking), the network schematisation (layered graph vs. graph or digraph) and including or excluding the pipe capacity.

2.10. Metrics applied to compare the outcomes of the Achilles approach and the GBWLM

In comparing the Achilles approach and the GBWLM, the following metrics are used:

- characteristics of the results:

  o Flooding volume of the storm sewer.
  o The number of flooded manholes at system level.
  o The locations of the flooded manholes.
  o The rise of the surface water level.

The results of the GBWLM are compared with the outcomes of a hydrodynamic storm sewer and surface water model serving as a reference.

The root mean squared error (RMSE) and correlation coefficient (R^2) are used to compare the outcomes of the hydrodynamic models and the GBWLM for the extent of flooding events (storm sewer component of the GBWLM) and increase of water levels (surface water component of the GBWLM). The Kendall rank correlation coefficient (Kendall 1945) commonly referred to as Kendall's tau-*b* coefficient (τ_b) is used to determine the relationship between the outcomes of the Achilles approach and those of the GBWLM. τ_b is a nonparametric measure of association based on the number of concordances and discordances in paired observations. τ_b can be interpreted as a measure of similarity between two data sets. Minus one (-1) implies a 100% negative association; one (1) is a 100% positive association. Equation (5) presents this calculation:

$$\tau_b = \frac{(P - Q)}{\left(\sqrt{(P + Q + X_0)*(P + Q + Y_0)}\right)} \tag{5}$$

where τ_b is Kendall's tau-*b* coefficient, *P* is the number of concordant pairs, *Q* is the number of discordant pairs, X_0 is the number of pairs tied only to the *X* variable and Y_0 is the number of pairs tied only to the *Y* variable.

Table 5 | Characteristics of the GTM for pressurised and gravity-driven systems

	Pressurised systems	Gravity-driven systems
Outcome	Ranking of the elements	Ranking of the elements
Network schematisation	Graph	Digraph
Costs of edges	Dynamic head loss	Static and dynamic head loss
Capacity of edges	Not applicable	Not applicable

Table 6 | Characteristics of the GBWLM for urban drainage systems consisting of gully pots, storm or combined sewer systems and surface water

	Gully pots	Storm sewer	Surface water
Outcome	Flooded area and flood frequency	Flooded area and flood frequency	Flooded area and flood frequency
Network schematisation	Not applicable	Digraph 3 layers	Digraph 2 layers
Costs of edges	Not applicable	Static and dynamic head loss	Static and dynamic head loss
Capacity of edges	Not applicable	Linearised hydraulics	Linearised hydraulics

The F_1 score (or F_1 measure) is a measure of the accuracy of a test. It combines the recall and precision in a single measure. The recall is a measure of the critical elements that were correctly identified as such and the precision represents the proportion of correctly identified critical elements. The following relations apply if recall and precision are of equal weight (Chinchor 1992):

$$F_1 = \frac{2*P*R}{P+R} = \frac{2*TP}{2*TP+FP+FN} \tag{6}$$

$$R = \frac{TP}{TP+FN} \tag{7}$$

$$P = \frac{TP}{TP+FP} \tag{8}$$

where P is precision (–), R is recall (–), TP is true positive (–), FP is false positive (–), FN is false negative (–) and F_1 is the F_1 score (–).

The precision of the GBWLM is the number of correctly identified flooded manholes divided by the total number of flooded manholes identified by the GBWLM. The recall of the GBWLM is the correctly identified number of flooded manholes by the GBWLM divided by all the flooded manholes (in the hydrodynamic model).

2.11. Case study details

A part of the urban water system in the municipality of Almere (the Netherlands) was used as a case study for testing the GBWLM. Almere is located in the province of Flevoland an entirely human-made and human-controlled polder system that was reclaimed from the former Zuiderzee. The case study focused on the surface water system in Almere Centrum (Figure 7) and the storm sewer catchments Waterwijk Oost Noord (referred to as Waterwijk Noord) and Waterwijk Oost Zuid (referred to as Waterwijk Zuid), situated in the north-eastern part of the area (see Table 7). The pumping station that discharges water to a larger regional surface water system is situated just to the south of Waterwijk Zuid.

Figure 7 | The urban water system of Almere.

The 'Weerwater' is a large pond (1.5 km^2) located in the centre of the surface water system. The Weerwater has a dampening effect on variations in the surface water level because of its storage capacity. The surface water system is divided into a main system and a smaller subsystem. The main system is directly connected to the storm water systems and has a water level of –5.5 m reference level. The reference water level in the smaller section in the southwestern part is –4.8 m, which defines a boundary condition for the main system. Water is discharged from the subsystem to the main system during storm events. The characteristics of the surface water system are summarised in Table 8.

Table 9 provides an overview of the runoff area per gully pot determined using the Voronoi triangulation (Voronoï 1908).

2.12. Applied rainfall series

For the analysis of urban water system networks and to understand the consequences of interactions between the subsystems and the perennial precipitation series were used. The applied rainfall series is the registered series by the Royal Dutch Meteorological Institute in De Bilt over the period 1955–1979 with a 15 min resolution.

Table 7 | The characteristics of the storm sewer systems in Waterwijk Noord and Waterwijk Zuid

Characteristics	Waterwijk Noord	Waterwijk Zuid
System type	Storm sewer	Storm sewer
Catchment area	Flat	Flat
System structure	Branched	Branched
Surface level (m reference level)	−4.00 and −2.43	−4.34 and −3.06
Contributing area (km^2)	0.15	0.09
Storage volume (mm/m^3)	1.73/253	0.83/76
Number of edges	118	92
Number of manholes	99	76
Outflow structure	3	4
Surface water level (m reference level)	−5.5	−5.5

Table 8 | The characteristics of the surface water system of Almere Centrum

Characteristics	Surface water system Almere Centrum
Length of channels (km)	39.8
Area surface water (km^2)	2.6
Runoff area unpaved (km^2)	8.0
Runoff area paved (km^2)	12.4
Surface water level (m reference level)	−4.8 and −5.5
Number of internal weirs	3
Number of culverts	12
Pump capacity (m^3/s)	3.41

Table 9 | The characteristics of the gully pots in Waterwijk Noord and Waterwijk Zuid

Characteristics	Waterwijk Noord	Waterwijk Zuid
Number gully pots	696	461
Average runoff surface per gully pot (m^2)	103	119
Maximum runoff surface per gully pot(m^2)	338	486

The rainfall includes an event with a return period of approximately 50–100 years (11–14 October 1960, 108.6 mm in 96 h). This implies that the rainfall series includes a representative event with a return period close to the design return period ($T =$ 100) of the surface water system, despite the series being relatively short.

The GBWLM was validated against the outcomes of a hydrodynamic surface water model and a hydrodynamic storm sewer model of Almere. The period 1955–1964 of the above-mentioned rainfall series was used for the validation of the surface water part of the GBWLM. A storm event with increasing rainfall intensity from 1 to 30 mm/h in steps of 1 mm/h was used for the validation of the storm sewer component. The duration of each precipitation intensity was 12 h to ensure (near) stationary conditions in the whole system. Between each of the two consecutive precipitation intensities, a dry period of 5 days was applied. This meant that the initial conditions at the different intensities were identical. The results of the GBWLM were compared with the results from a hydrodynamic model for these 30 storm intensities.

3. CASE STUDY RESULTS, THEIR INTERPRETATION AND DISCUSSION

3.1. Results of the case study of the GBWLM

Flood frequency and flood extent were used to analyse the impact of capacity reduction on the urban water system of Almere. The flood frequency and extent were determined for various capacity reductions of the three analysed subsystems: gully pots, storm sewer and surface water. The results are presented in bar charts (Figures 8 and 9); the horizontal axis shows the applied capacity reduction (%), the vertical axis shows the resulting flood frequency (number per year) and the bar colour indicates the flood extent (flooded area as a percentage of total paved area).
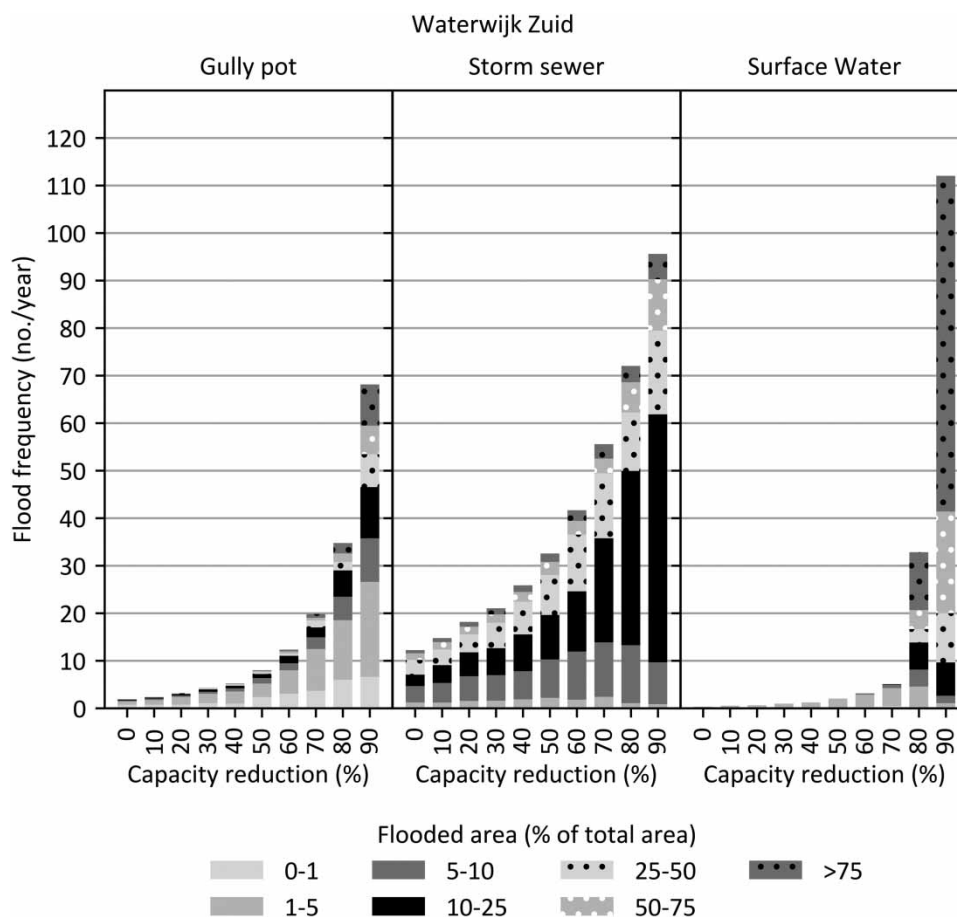

Figure 8 | Overview of the yearly flood frequency for the various available capacities of gully pots, storm sewers and surface water system in Waterwijk Zuid. The flood frequency of the gully pots is 2 times per year the flood frequency of the storm sewer 12 times per year and the flood frequency of the surface water is less than 1 time/year if full capacity is available.
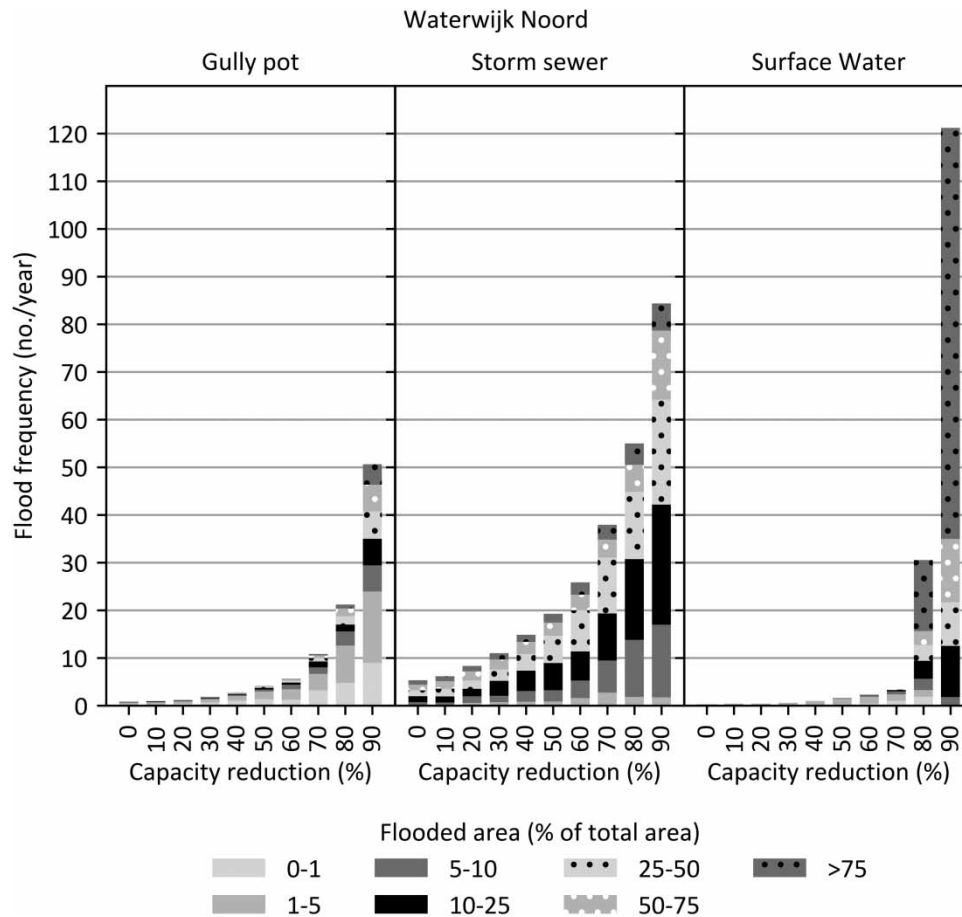
Waterwijk Noord

Figure 9 | Overview of the flood frequency per year for the various available capacities of gully pots, storm sewers and surface water system in Waterwijk Noord. The flood frequency of the gully pots is less than 1 time per year, the flood frequency of the storm sewer 5 times per year and the flood frequency of the surface water is less than 1 time/year if full capacity is available.

The results for the surface water network in Figures 8 and 9 present the increase of flooding compared to the reference situation in which all three subsystems have full capacity. The total flooding is therefore the sum of the flood in the storm sewer at 0% capacity reduction and the flood due to the surface water system.

3.1.1. Gully pots

The performance of the gully pots in Waterwijk Zuid and Noord at declining capacity was similar. However, both the flood frequency and flood extent were larger in Waterwijk Zuid. This corresponds with the (approximately 15%) larger average runoff area per gully pot in Waterwijk Zuid (see Table 9). The flood frequencies of the gully pots were 0–2 times per year, if full capacity was available.

The flood frequency and flood extent increased in a non-linear relationship with decreasing capacity. The impact on the performance was limited for capacity reductions up to 40%. The flood frequency was 5 or 6 times per year and the flood extent was limited to 5% of the area for most events. This implies that the overcapacity for most gullies was approximately 30%. This can be considered a safety factor in the design.

3.1.2. Surface water

A reduction in the discharge capacity of the surface water system had a slightly greater impact on the frequency and extent of flooding in Waterwijk Noord than in Waterwijk Zuid. At the full capacity of the surface water system, the flood frequency was less than once a year. The impact of a capacity reduction of the surface water was relatively limited when the capacity

reduction was limited to 70%. Both the flood frequency and flooded area increased strongly with an increased capacity reduction.

The number of times that more than 75% of the surface was flooded was approximately 85 times per year in Waterwijk Noord and 70 times per year in Waterwijk Zuid in the case of a capacity reduction of 90%. This is notable because Waterwijk Noord floods less frequent than Waterwijk Zuid for capacity reductions up to 80%.

3.1.3. Storm sewer

The differences in the performance of the two storm sewer systems were larger than those of the other subsystems in the two catchments. Waterwijk Zuid flooded about 12 times a year and Waterwijk Noord five times a year without capacity reduction. More events with a small flood extent occurred in Waterwijk Zuid than in Waterwijk Noord. The flood frequency increased to 96 times per year in Waterwijk Zuid and 85 times per year in Waterwijk Noord if the capacity declined.

The most striking difference was observed in the extent of flooding. A clear increase could be seen in the frequency of events with a flood extent of 10–25% in Waterwijk Zuid if the capacity decreased. In Waterwijk Noord, the frequency of all flood extent categories increased. This means that a decrease in the capacity of the storm sewer in Waterwijk Zuid resulted in higher flood frequencies, but to a limited extent. In Waterwijk Noord, both smaller and larger flood events occurred more frequently.

The three subsystems are analysed in an integrated manner using the GBWLM. This allows the spatial and temporal resolutions of the models to be aligned. This is often a problem when integrating individual models into an integrated model (Tscheikner-Gratl et al. 2019). The computational effort required is reduced because the GBWLM uses flow path analysis instead of hydrodynamic models. This allows precipitation series to be applied instead of events, as in the Achilles approach (Mair et al. 2012).

Event selection in advance is difficult due to the differences in storage and drainage characteristics of subsystems. The combination of storage and discharge capacity determines the time it takes for the system to return to its initial status after a storm event. Therefore, it is not possible to apply design events with a known return period to integrated systems. A multiyear analysis is necessary for a reliable static analysis of the probability of flooding (Vaes et al. 2009). Therefore, we used a 25-year series applying a 25-year precipitation series in the GBWLM case study shows that event selection is not necessary.

3.2. Validation of the GBWLM

The results of the GBWLM were validated against the Achilles approach. The validation was based on four criteria:

1. Flood volume at the system level of the storm sewer.
2. Number of flooded manholes at system level.
3. Locations of flooded manholes.
4. Rise of the surface water level.

A storm event was used with a progressive rainfall intensity ranging from 1 to 30 mm/h to validate the storm sewer system of the GBWLM. A dry period of 5 days was applied between each of the two consecutive precipitation intensities. Thus, the initial conditions at the different intensities were identical. The results are summarised in Table 10 (for more details, see supplementary material). The table shows the minimum values of the 30 events.

The correlation between the flood volume of the Achilles approach and GBWLM for the storm sewer was significant ($R^2 =$ 0.97–0.98 and $\tau_b = 0.95$–0.96, supplementary material Figure S2). This implies a high degree of equality in the flood volume outcomes according to the Achilles approach and the GBWLM.

The flooding started at a slightly lower rainfall intensity (2 mm/h) in the GBWLM when compared to the Achilles approach, while the GBWLM provide a satisfactory estimate for both the total number of flooded manholes and the locations where the flooding occurs (Figures S3–S6, supplementary material). The scores for the number of flood locations and the locations of the flooded manholes were lowest at the transition between non-flooded and flooded regions. The percentage of correctly classified manholes (flooded, non-flooded) reached the lowest score of 72% correctly classified manholes. In this transition phase, the indicator for the locations of flooded manholes, the F_1 score, may drop below 0.3. The F_1 score is low because only a few manholes were flooded in the transitional phase. The impact on the F_1 score is significant if some of these manholes are not correctly classified. The F_1 score increased rapidly if the rain intensity after the transition between non-flooded and flooded increased by 2 mm/h.

Table 10 | Overview of the validation results for the GBWLM for a sewer system, based on a storm event with an increasing intensity of 1–30 mm/h

		Waterwijk	Waterwijk Zuid	Waterwijk Noord
Flood volume	R^2	0.98	0.98	0.97
	τ_b	0.95	0.95	0.96
Flooded manholes	True positive/negative (minimum%)	84	69	82
	False positive (maximum%)	12	21	6
	False negative (maximum%)	6	14	18
F_1 (overall)	F_1	0.84	0.87	0.8
	Precision	0.78	0.84	0.7
	Recall	0.90	0.90	0.92
F_1 (minimum value)	F_1	0.21	0.24	0.11
	Precision	0.16	0.19	0.06
	Recall	0.33	0.33	0.84

The values of the flooded manholes and the F_1 score are the minimum values of the 30 events.

The surface water system was validated with a 10-year rainfall series and the water level variation of the GBWLM was compared with the results of the Achilles approach. The results of the validation of the surface water part of the GBWLM showed a strong correlation with the results of the Achilles approach ($R^2 = 0.93$; see supplementary material, Figure S7). This means that the GBWLM followed the pattern of surface water level rise in the Achilles approach.

3.3. Applicability of the GBWLM at increased rainfall intensities

The performance of networks can be affected as a result of either a change in load or capacity of the networks (Reyes-Silva *et al.* 2020). The case study of Almere focused on the decrease in capacity of subsystems. This subsection shows that the consequences of an increase in load are similar to those of a decrease in capacity.

A comparison was made between the freeboard (freeboard is the distance between ground level and water level) at a doubling of the precipitation intensity and at a halving of the discharge capacity for a storm sewer system. Three sets of calculations were performed:

1. The storm sewer system was tested with two stationary events of 4 and 8 mm/h.
2. The intensity of the events was doubled and the storm sewer system was tested with two stationary events of 8 and 16 mm/h.
3. The discharge capacity of the storm sewer system was halved and tested with two stationary events of 4 and 8 mm/h.

The storm sewer network reacted similarly to a capacity reduction of the pipe diameter and increased storm intensity. Figure 10 shows that when the storm intensity increased by a factor of two (Figure 10, bottom-left) or the available capacity decreased by a factor of two (Figure 10, bottom-right), the changes in freeboard were as expected and of the same order of magnitude (Figure 10, top-right). This means that the GBWLM can be used to analyse the impact of both a decrease in capacity of the system and an increase in load on the system.

The rainfall intensities of storm events with return periods of 0.5–1,000 years and duration of 10 min–12 h are expected to increase by 17.1–21.3% as a result of climate change (Beersma *et al.* 2019). This is expected to correspond to a capacity reduction of approximately 20% (Figure 10). Figures 8 and 9 show that such a capacity reduction had little impact on the flood frequency and extent caused by gully pots and surface water. However, it could lead to a 50% increase in the storm sewer flood frequency and an increase in the extent of flooding.

3.4. Required input data and effort

The GBWLM is more accessible than the Achilles approach (Möderl *et al.* 2009; Mair *et al.* 2012) because fewer data and less computational effort are needed. The computational effort required for the Achilles approach is approximately 30 times greater than that for the GBWLM.

Correct representation of the network structure and geometry is important in both approaches; however, hydrodynamic models are replaced by path analysis of digraphs in the GBWLM. The GBWLM requires less information about manholes and structures when compared to the Achilles approach.
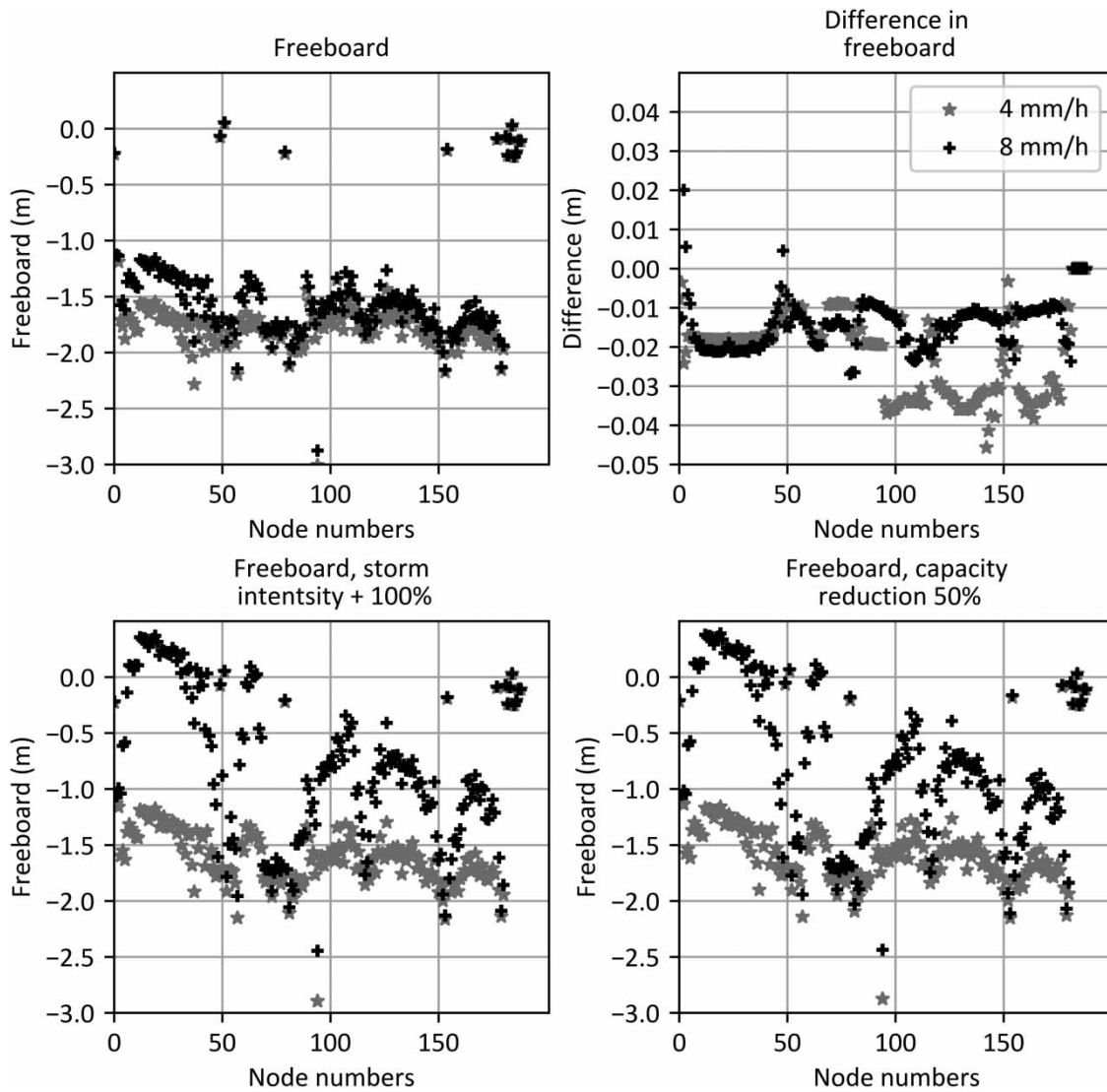
Table 11 shows the data not included in the GBWLM.

Figure 10 | Comparison of the freeboard in the event of an increase of the storm intensity and a decrease of the available capacity for a storm event of 4 and 8 mm/h. *Note*: A different *Y*-scale has been used for the graph top-right.

Collecting data regarding structures normally may require a significant effort, particularly when the sewer must be accessed to obtain these data. Information about manholes can be collected relatively easily and is often combined with sourcing characteristics that are necessary for both the Achilles approach and the GBWLM.

Table 11 | Overview of the required data per sub system included in hydrodynamic models and excluded in the GBWLM

Rainfall-runoff models	Gully pots	Storm sewers	Surface water system
Runoff parameters	Inlet parameters	Street level manhole	Thalweg (centre line of the water system)
Differentiation of roof types	*z*-coordinate	Dimensions manholes	Cross sections
Differentiation of paved area types		Weir characteristics (except height)	Weir characteristics (except capacity)
Differentiation of unpaved area types		Pump characteristics (except capacity)	Pump characteristics (except height)

3.5. Limitations of the GBWLM

The most important limitation of the GBWLM is that the method is not fully applicable to all urban drainage systems. Its applicability depends on the linearisation potential of the hydraulics. If the hydraulic gradients are heterogenic, the results of the GBWLM will differ more from the results of hydrodynamic models. Meijer *et al.* (2022) present the Network Linearisation Parameter (NLP) to get a first indication or the GBWLM can be applied successfully. Possibly, linearisation based on the pipe gradient or the ground level gradient may increase the scope of application of the GBWLM in sloping areas.

4. CONCLUSIONS

The GBWLM differs from the Achilles approach in that the former relies on network structure and flow path analysis, while the latter requires the application of full hydrodynamics. The advantages of the GBWLM approach can be summarised as:

- A full and integrated analysis of urban drainage systems (gully pots, storm sewers and surface water).
- An analysis with a full (multiyear) rainfall series consisting of multiple events.
- Less required computational effort, resulting in a significant reduction of simulation run times. At the price of a simplification of the representation of the hydrodynamics (in GBWLM, this is linearised).
- Determination of the effects of both reduced (sub)system capacity and increased rainfall intensities.

The parameters 'flood extent' and 'flood frequency' were used to assess the system's performance. Both are indicators for the severity of floods and can be used as a basis to determine the consequences in terms of impact, such as damage or health risk.

The outcomes of the analysis can be used to prioritise maintenance activities and system rehabilitation. Our results showed that the storm sewer system of Almere Waterwijk is the weakest link and most prone to capacity reduction. The flood frequency may increase by approximately 50% in 2050 as a consequence of climate change.

The case study also showed that the GBWLM is applicable for systems where the functioning is determined by both discharge and storage capacity. This means that many different types of systems could be analysed with the GBWLM. This research may contribute to the analysis of larger networks with other parameters, such as concentration times. This can allow for an analysis of large river systems with the GBWLM that, over time could help to optimise the design and maintenance of these systems.

DATA AVAILABILITY STATEMENT

All relevant data are included in the paper or its Supplementary Information.

CONFLICT OF INTEREST

The authors declare there is no conflict.

REFERENCES

Bach, P. M., Rauch, W., Mikkelsen, P. S., McCarthy, D. T. & Deletic, A. 2014 A critical review of integrated urban water modelling – urban drainage and beyond. *Environmental Modelling & Software* **54**, 88–107. https://doi.org/10.1016/j.envsoft.2013.12.018.

Beersma, J., Hakvoort, H., Jilderda, R., Overeem, A. & Versteeg, R. 2019 *Neerslagstatistiek en -reeksen voor het waterbeheer 2019 [Rainfall Statistics and Series for Water Management 2019] (STOWA Report No. 2019-19)*. Stichting Toegepast Onderzoek Waterbeheer. Available

from: https://www.stowa.nl/sites/default/files/assets/PUBLICATIES/Publicaties%202019/STOWA%202019-19%20neerslagstatistieken.pdf

Broadbent, S. R. & Hammersley, J. M. 1957 Percolation processes: I. Crystals and mazes. *Mathematical Proceedings of the Cambridge Philosophical Society* **53** (3), 629–641. https://doi.org/10.1017/S0305004100032680.

Chinchor, N. 1992 MUC-4 evaluation metrics. In: *MUC4 '92: Proceedings of the 4th Conference on Message Understanding*. Association for Computational Linguistics, pp. 22–29. https://doi.org/10.3115/1072064.1072067.

Dijkstra, E. W. 1959 A note on two problems in connexion with graphs. *Numerische Mathematik* **1** (1), 269–271. https://doi.org/10.1007/BF01386390.

Ferguson, C. R. & Fenner, R. A. 2020 The potential for natural flood management to maintain free discharge at urban drainage outfalls. *Journal of Flood Risk Management* **13** (3). https://doi.org/10.1111/jfr3.12617.

Fischer, A., Rouault, P., Kroll, S., Van Assel, J. & Pawlowsky-Reusing, E. 2009 Possibilities of sewer model simplifications. *Urban Water Journal* **6** (6), 457–470. https://doi.org/10.1080/15730620903038453.

Geels, F. W. 2006 The hygienic transition from cesspools to sewer systems (1840–1930): the dynamics of regime transformation. *Research Policy* **35** (7), 1069–1082. https://doi.org/10.1016/j.respol.2006.06.001.

Hagberg, A. A., Schult, D. A., Swart, P. J., 2008 Exploring network structure, dynamics, and function using NetworkX. In: *Proceedings of the 7th Python in Science Conference (SciPy2008)* (Varoquaux, G., Vaught, T. & Millman, J., eds), pp. 11–15. SciPy Conference – Pasadena, CA

Kendall, M. G. 1945 The treatment of ties in ranking problems. *Biometrika* **33** (3), 239–251. https://doi.org/10.2307/2332303.

Kourtis, I. M. & Tsihrintzis, V. A. 2021 Adaptation of urban drainage networks to climate change: a review. *Science of The Total Environment* **771**, 145431. https://doi.org/10.1016/j.scitotenv.2021.145431.

Langeveld, J. & Schilperoort, R. 2019 Stedelijk Water 2040: hemelwater verbindt! [Urban water 2040: Rainwater connects!] [White paper]. Partners4UrbanWater. Available from: https://www.urbanwater.nl/Files/190604_Whitepaper_hemelwater_verbindt.pdf

Mair, M., Sitzenfrei, R., Kleidorfer, M., Möderl, M. & Rauch, W. 2012 GIS-based applications of sensitivity analysis for sewer models. *Water Science & Technology* **65** (7), 1215–1222. https://doi.org/10.2166/wst.2012.954.

Meijer, D., Van Bijnen, M., Langeveld, J., Korving, H., Post, J. & Clemens, F. 2018 Identifying critical elements in sewer networks using graph-theory. *Water* **10** (2), 136. https://doi.org/10.3390/w10020136.

Meijer, D., Post, J., Van der Hoek, J. P., Korving, H., Langeveld, J. & Clemens, F. 2020 Identifying critical elements in drinking water distribution networks using graph theory. *Structure and Infrastructure Engineering* **17** (3), 347–360. https://doi.org/10.1080/15732479.2020.1751664.

Meijer, D., Korving, H. & Clemens-Meyer, F. 2022 A topological characterisation of looped drainage networks. *Structure and Infrastructure Engineering* 1–14. https://doi.org/10.1080/15732479.2022.2152464.

Möderl, M., Kleidorfer, M., Sitzenfrei, R. & Rauch, W. 2009 Identifying weak points of urban drainage systems by means of VulNetUD. *Water Science & Technology* **60** (10), 2507–2513. https://doi.org/10.2166/wst.2009.664.

NetworkX Developers n.d. min_cost_flow. NetworkX. Available from: https://networkx.org/documentation/stable/reference/algorithms/generated/networkx.algorithms.flow.min_cost_flow.html

Preston, S. H. & van de Walle, E. 1978 Urban French mortality in the nineteenth century. *Population Studies* **32** (2), 275–297. https://doi.org/10.2307/2173562.

Qiang, Y., Zhang, L., He, J., Xiao, T., Huang, H. & Wang, H. 2021 Urban flood analysis for Pearl River delta cities using an equivalent drainage method upon combined rainfall-high tide-storm surge events. *Journal of Hydrology* **597**, 126293. https://doi.org/10.1016/j.jhydrol.2021.126293.

Reyes-Silva, J. D., Helm, B. & Krebs, P. 2020 Meshness of sewer networks and its implications for flooding occurrence. *Water Science & Technology* **81** (1), 40–51. https://doi.org/10.2166/wst.2020.070.

Sahimi, M. 1994 *Applications of Percolation Theory*. Abingdon, United Kingdom: Taylor & Francis.

Sommer, T., Karpf, C., Ettrich, N., Haase, D., Weichel, T., Peetz, J. V., Steckel, B., Eulitz, K. & Ullrich, K. 2009 Coupled modelling of subsurface water flux for an integrated flood risk management. *Natural Hazards and Earth System Sciences* **9** (4), 1277–1290. https://doi.org/10.5194/nhess-9-1277-2009.

Stauffer, D. & Aharony, A. 1991 *Introduction to Percolation Theory* (Rev. 2nd ed.). Taylor & Francis. https://doi.org/10.1201/9781315274386

Stockmayer, W. H. 1944 Theory of molecular size distribution and gel formation in branched polymers: II. General cross linking. *The Journal of Chemical Physics* **12** (4), 125–131. https://doi.org/10.1063/1.1723922.

Tscheikner-Gratl, F., Bellos, V., Schellart, A., Moreno-Rodenas, A., Muthusamy, M., Langeveld, J., Clemens, F., Benedetti, L., Rico-Ramirez, M. A., Fernandes de Carvalho, R., Breuer, L., Shucksmith, J., Heuvelink, G. B. M. & Tait, S. 2019 Recent insights on uncertainties present in integrated catchment water quality modelling. *Water Research* **150**, 368–379. https://doi.org/10.1016/j.watres.2018.11.079.

Vaes, G., Feyaerts, T. & Swartenbroekx, P. 2009 Influence and modelling of urban runoff on the peak flows in rivers. *Water Science & Technology* **60** (7), 1919–1927. https://doi.org/10.2166/wst.2009.638.

van Riel, W. 2016 *On Decision-Making for Sewer Replacement*. Doctoral Thesis, Delft University of Technology, TUDelft. https://doi.org/10.4233/uuid:92b10448-795d-43ac-8071-d779af9d374d

Voronoï, G. 1908 Nouvelles applications des paramètres continus à la théorie des formes quadratiques : Deuxième mémoire : Recherches sur les parallélloèdres primitifs [New applications of continuous parameters to the theory of quadratic forms: second dissertation: research

on primitive paralleloids]. *Journal für die reine und angewandte Mathematik* **1908** (134), 198–287. https://doi.org/10.1515/crll.1908. 134.198.

Yang, Q., Dai, Q., Han, D., Zhu, X. & Zhang, S. 2018 Impact of the storm sewer network complexity on flood simulations according to the stroke scaling method. *Water* **10** (5), 645. https://doi.org/10.3390/w10050645.

Zounemat-Kermani, M., Matta, E., Cominola, A., Xia, X., Zhang, Q., Liang, Q. & Hinkelmann, R. 2020 Neurocomputing in surface water hydrology and hydraulics: a review of two decades retrospective, current status and future prospects. *Journal of Hydrology* **588**, 125085. https://doi.org/10.1016/j.jhydrol.2020.125085.